

Effect of Thermal Treatment on the Intermetallic Compounds Formed at Sn-9Zn-1.5Ag-xBi (x = 0 and 1) Lead-Free Solder/Cu Interface

Chih-Yao Liu¹, Ying-Ru Chen², Wang-Long Li^{2,3}, Min-Hsiung Hon¹ and Moo-Chin Wang^{4,*}

¹Department of Materials Science and Engineering, National Cheng Kung University,
1 Ta-Hsueh Road, Tainan, 70101, Taiwan, R. O. China

²Department of Mechanical Engineering, National Kaohsiung University of Applied Sciences,
415 Chien-Kung Road, Kaohsiung 80782, Taiwan, R. O. China

³Institute of Nanotechnology and Microsystems Engineering, National Cheng Kung University,
1 Ta-Hsueh Road, Tainan, 70101, Taiwan, R. O. China

⁴Faculty of Fragrance and Cosmetics, Kaohsiung Medical University,
100, Shihchuan 1st Road, Kaohsiung, 80728, Taiwan, R. O. China

The formation of Intermetallic compounds (IMCs) at the interface between an Sn-9Zn-1.5Ag-xBi solder alloy and a Cu substrate dipped at 250°C and heat-treated at 150°C for various times has been investigated by an optical microscope (OM), an X-ray diffractometer (XRD) and a scanning electron microscope (SEM) with an energy dispersive spectrometer (EDS). The OM result shows the flat and smooth surface for the Sn-9Zn-1.5Ag-1Bi solder alloy and Cu substrate after dipping at 250°C. The phases of IMCs formed are Cu₆Sn₅ and Cu₅Zn₈ for both lead-free solder alloys. After thermal treatment at 250°C for 200 h, the phases of IMCs are Cu₆Sn₅, Cu₅Zn₈ and Ag₃Sn. The Cu₆Sn₅ has a scallop morphology, and is located at the interface between the solder and Cu substrate. The adhesion strength for the Sn-9Zn-1.5Ag-1Bi lead-free solder alloy is higher than the Sn-9Zn-1.5Ag solder alloy. After being heat-treated at 150°C, the adhesion strength of the Sn-9Zn-1.5Ag-1Bi solder alloy decreases from 12.67 ± 0.45 to 6.92 ± 0.38 MPa after thermal treatment for 200 h. [doi:10.2320/matertrans.MRA2007075]

(Received March 28, 2007; Accepted May 14, 2007; Published July 4, 2007)

Keywords: lead-free solder, microstructure, morphology, Cu₆Sn₅, adhesion strength

1. Introduction

For electronic parts and devices, solder joints provide electrical conductivity and suitable mechanical strength.¹⁾ Although a lot of solder alloys can be chosen, a eutectic Sn-Pb solder alloy with 37–40 mass% lead is used for soldering in electronic assemblies due to its excellent wettability and other necessary properties such as melting temperature and adhesion strength. However, Sn-37Pb solder alloy applications in the electronic packing industry are limited because of its toxicity and the risks of ground water pollution.^{2,3)} Major industrial countries such as the United States, Japan and the European Community have established policies that indicate a shift to lead-free processes, resulting in more research on lead-free solders in the electronic industry to replace the Pb-Sn system.⁴⁾

Sn-9Zn and Sn-3.5Ag are the two important binary lead-free solders,^{5,6)} however, the inferior wettability and oxidation resistance of an Sn-9Zn solder alloy and high melting point (221°C) of an Sn-3.5Ag alloy limit their usage.^{7,8)} Takemoto and Funaki⁹⁾ have shown that Ag addition to an Sn-9Zn solder alloy can improve wettability between solder alloy and Cu substrate, because Ag addition reduces the potential difference between a base metal and a solder alloy. Chang *et al.*¹⁰⁾ have pointed out that the solidus temperature of an Sn-9Zn-xAg solder alloy is 197°C and this decreases from 225.3°C to 221.7°C and 223.6°C as Ag addition is increased from 1.5 to 2.5 and 3.5 wt%, respectively. Moreover, Ag addition offers better solder joint reliability and hinders the formation of Kirkendall voids, as demonstrated by Chang *et al.*¹⁰⁾

In the practical packaging process, the pasty temperature range between solid and liquid phases affects the wettability and IMCs thickness.^{11,12)} Smaller pasty temperature range leads to shorter reaction time between solid and liquid. However, the pasty temperature for Sn-9Zn-xAg alloys (x = 1.5 to 3.5 mass%) ranges from 28.3°C to 26.6°C, which is not small enough for a candidate solder alloy. Therefore, addition of other alloy elements to Sn-Zn-Ag solder alloys for reducing the pasty temperature is one way to overcome this issue. In fact, Liu *et al.*¹³⁾ have demonstrated that addition of 0.5 mass% Bi to a Sn-9Zn-1.5Ag solder can reduce the melting temperature and pasty range, because the melting point of Bi is lower than Sn, Zn and Ag. In addition, the solidus and liquidus temperatures for Sn-9Zn-1.5Ag-0.5Bi are 197 and 207°C, respectively.¹³⁾

In this study, the effect of thermal treatment in the intermetallic compounds formed at the interface between Sn-9Zn-1.5Ag-xBi lead-free solder alloy and Cu substrate have been investigated using optical microscopy (OM), X-ray diffraction (XRD), and scanning electron microscopy (SEM) with energy dispersive spectrometry (EDS). The purpose of this investigation is (i) to determine the phases of the IMCs formed at the Sn-9Zn-1.5Ag-xBi/Cu interface as dipped and heat treated at 150°C for various times and (ii) to evaluate the effect of thermal treatment time on the adhesion strength of Sn-9Zn-1.5Ag-xBi solder alloys.

2. Experimental Procedure

2.1 Sample preparation

The Sn-9Zn-1.5Ag and Sn-9Zn-1.5Ag-1Bi solder alloys (in mass%) were prepared by melting pure Sn, Zn, Ag and Bi (purity > 99.9%). Each pure metal was deoxidized with a

*Corresponding author, E-mail: mcwang@kmu.edu.tw

5 vol% HCl solution at ambient temperature and degreased with a 5 mass% NaOH solution at 70°C. For the Sn-9Zn-1.5Ag solder alloy, pure Sn, Zn and Ag were melted at 600°C in a stainless steel crucible and stirred to homogenize the mixture. The melted solder alloy was cast in a metal mold with a diameter of 3 cm at 250°C and cooled in air.

For the Sn-9Zn-1.5Ag-1Bi solder alloy, pure Sn, Zn and Ag were also melted at 600°C in a stainless steel crucible and stirred to homogenize the mixture. When the melted alloy was cooled to 300°C and the dross was removed, pure Bi (99.9%) was added to the melted alloy and stirred in. Subsequently, the melt was cast in a metal mold with a diameter of 3 cm at 250°C and cooled in air. An oxygen-free, high-conductivity Cu plate with a size of 70 mm × 25 mm × 2 mm was used as a substrate and cleaned with the same procedure as described before. After pretreating, the Cu substrate was fluxed in a 3.5 mass% DMAHCl solution (3.5 wt% dimethylammonium chloride dissolved in ethanol) for 10 s to enhance activity and avoid reoxidizing of the surface. Subsequently, the Cu substrate was immersed in the molten Sn-9Zn-1.5Ag and Sn-9Zn-1.5Ag-1Bi, respectively, at 250°C for 60 s at a dipping rate of 11.8 mm/s to obtain a flat surface. The experimental detail has been described in our previous study.¹³⁾

After this dipping procedure, the samples were heat treated at 150°C for various times. The heat-treated sample was cross-sectioned, ground and polished with sandpapers and 0.3 μm Al₂O₃ powders. Finally, it was etched with 2 vol% HCl + 3 vol% HNO₃ + 95 vol% C₂H₅OH solution in order to determine the IMCs which formed at the interface between the solder and Cu substrate.

2.2 Sample characterization

The interface morphology of the solder alloy after dipping was determined with an optical microscope (OM). An X-ray diffractometer (XRD, D-MAX IIIB, Rigaku, Japan) was used to identify the IMCs formed at the interface, at a scanning rate of 2°/min from 20° to 80°. The interfacial morphology of the solder alloy/Cu interface was observed by SEM (JXA-840, JEOL, Japan), and EDS (AN10000/85S, LINKS, England) was used to determine the chemical composition of the IMCs. After heat treatment at 150°C for various times, twenty samples were deoxidized and degreased with sandpaper and acetone, respectively, and then attached to Al studs with a diameter of 0.275 cm. The adhesion strength was measured with a pull-off tester as demonstrated in our previous study.¹³⁾ The force was applied to an Al stud with a rate of 89.0 N/s. The adhesion strength, the fracture force divided by the area of the stud, was calculated by a computer.

3. Results and Discussion

3.1 Interface morphology of the Sn-9Zn-1.5Ag-xBi (x = 0 and 1) lead-free solder dipped at 250°C

Figure 1(a) shows the interface morphology of the Sn-9Zn-1.5Ag solder alloy dipped at 250°C for 60 s, indicating incomplete soldering. The interface morphology of the Sn-9Zn-1.5Ag-1Bi dipped at 250°C for 60 s is demonstrated in Fig. 1(b), indicating that a flat dipping surface of the Sn-9Zn-1.5Ag-1Bi is obtained with a coverage of 95%. The Sn-9Zn-

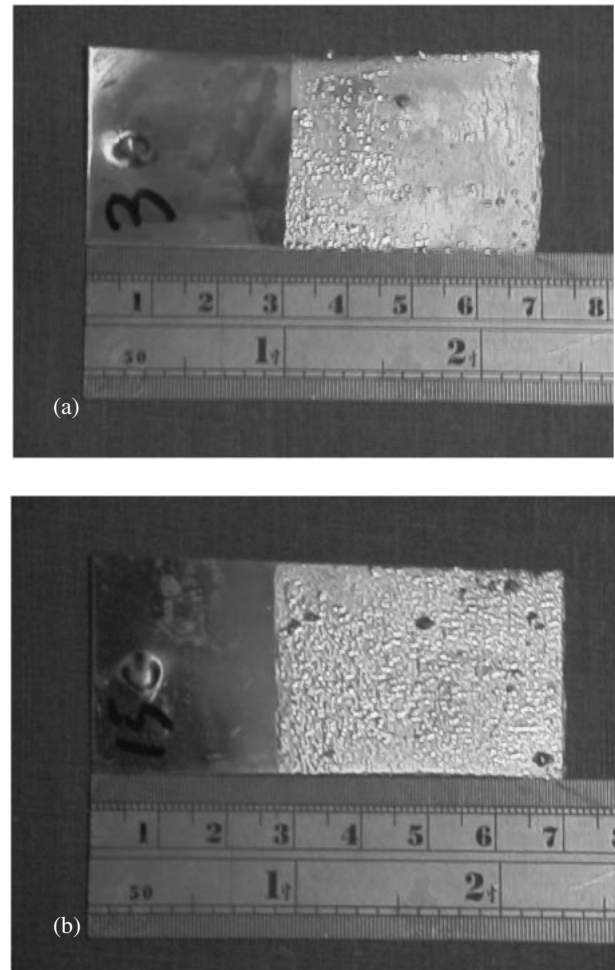


Fig. 1 Optical micrograph of (a) Sn-9Zn-1.5Ag solder alloy and (b) Sn-9Zn-1.5Ag-1Bi alloy dipped with Cu substrate at 250°C for 60 s.

1.5Ag-1Bi lead-free solder alloy has a better wettability due to Bi addition, which increases the mobility of the solder alloy on the Cu substrate. Our previous study¹³⁾ shows that the 0.5 mass% Bi addition to the Sn-9Zn-1.5Ag solder alloy has a better effect than no Bi addition. In fact, alloy mobility is a key point in the dipping process. In the present study, the temperature of 250°C is satisfactory for Sn-9Zn-1.5Ag-1Bi/Cu dipping.

While high soldering temperature increases the mobility of a solder alloy on a Cu substrate, it tends to accumulate, causing more heat on the substrate. For an industrial flip chip, there are many integrated circuit (IC) devices on the substrate and reflow occurs many times, and thus high heat accumulation reflow damages the flip chip and causes IC devices to fail. Therefore, the lower the soldering temperature, the better wettability for the Sn-9Zn-1.5Ag-1Bi solder alloy.

Moreover, the dipping temperature and time are other factors to influence the wettability of a solder alloy on a Cu substrate. Chang *et al.*¹²⁾ have demonstrated that the long dipping time increases the diffusion rate of a solder on a Cu substrate. In this study, the dipping time is 60 s and reflow time of the solder with the substrate is 2–3 minutes, so the dipping time increases from 60 s to 180 s. However, as the dipping time increases the formation of IMCs may also increase and cause complication at the interface.¹⁴⁾ This is not

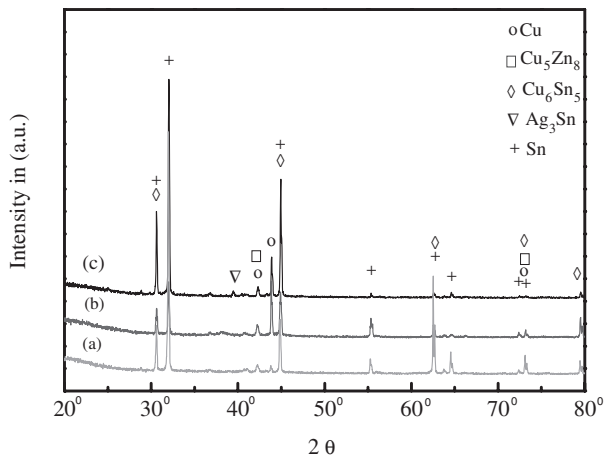


Fig. 2 XRD patterns of Sn-9Zn-1.5Ag solder alloy dipped with Cu substrate at 250°C for 60 s and heat-treated at 150°C for various times: (a) as-dipped, (b) 100 h and (c) 200 h.

good for the adhesion strength of solder/substrate interfaces, because dipping time affects IMCs thickness. When the IMCs thickness is larger, the adhesion strength is decreased. The ideal thickness of IMCs is about 3–5 μm .¹⁵⁾ Therefore, it is important to control dipping time and temperature.

3.2 IMCs formation at the interface between Sn-9Zn-1.5Ag-xBi (x = 0 and 1) solder alloy and Cu substrate when dipped at 250°C for 60 s.

Figure 2 shows the XRD patterns of the Sn-9Zn-1.5Ag solder alloy when dipped on the Cu substrate at 250°C and heat treated at 150°C for various times. Figure 2(a) indicates that the phases formed at the interface between the Sn-9Zn-1.5Ag alloy and Cu substrate are Cu_6Sn_5 and Cu_5Zn_8 . This result is caused by the Cu diffusing to the solder and reacting with Sn, forming Cu_6Sn_5 , and Zn diffusing to Cu, forming Cu_5Zn_8 , and thus these IMCs affect the adhesion strength and wettability on the Cu substrate. After being heat-treated at 150°C for 100 h, Fig. 2(b), the phases of IMCs are the same as Fig. 2(a). After being heat-treated at 150°C for 200 h, see Fig. 2(c), Ag_3Sn is also formed at the solder/substrate interface.

Figure 3 shows the XRD patterns of Sn-9Zn-1.5Ag-1Bi solder alloy when dipped on the Cu substrate at 250°C and heat treated at 150°C for different times. Figure 3(a) is as-soldered, indicating that Cu_6Sn_5 and Cu_5Zn_8 are formed at the solder/substrate interface. After being heat-treated at 150°C for 100 and 200 h, see Fig 3(b) and (c), respectively, in addition to Cu_6Sn_5 and Cu_5Zn_8 , Ag_3Sn is also formed at the interface.

The crystallite size is determined from the XRD pattern by using Scherer's equation:¹⁵⁾

$$D_{\text{hkl}} = \frac{0.9\lambda}{\beta_{\text{hkl}} \cos \theta}$$

where D_{hkl} is the crystallite size, λ is the wavelength of Cu $K\alpha = 0.15418 \text{ nm}$, θ is the reflection angle and β_{hkl} is the full width at half maximum (FWHM). Figure 4 is the relation between the crystallite size of Cu_6Sn_5 and heat-treatment times at 150°C. It shows that the crystallite size of Cu_6Sn_5 at

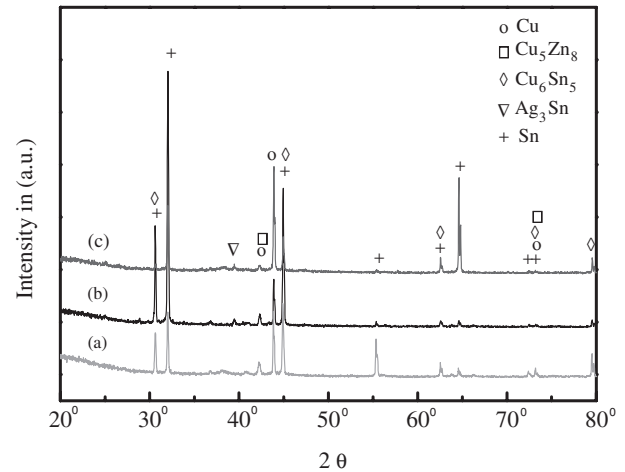


Fig. 3 XRD patterns of Sn-9Zn-1.5Ag-1Bi solder alloy dipped with Cu substrate at 250°C for 60 s and heat-treated at 150°C for various times: (a) as-dipped, (b) 100 h and (c) 200 h.

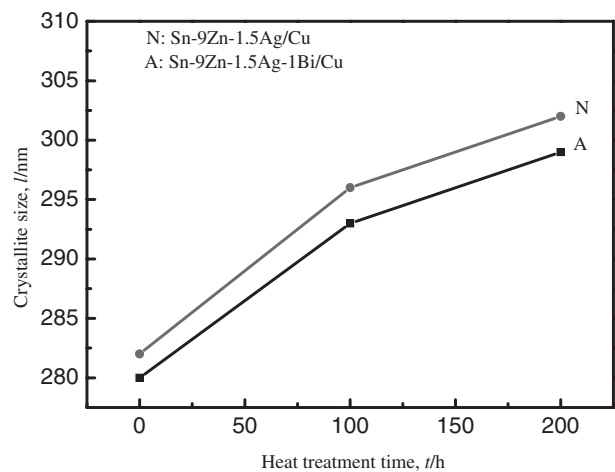


Fig. 4 Grain size of Sn-9Zn-1.5Ag-xBi/Cu heat-treated at 150°C for various times.

the Sn-9Zn-1.5Ag-xBi/Cu interface is the largest when heat-treated for 200 h. Figure 5(a) shows the IMCs morphology of the Sn-9Zn-1.5Ag/Cu when dipped at 250°C for 60 s. The phases of IMCs are Cu_6Sn_5 and Cu_5Zn_8 . The scallop-shaped Cu_6Sn_5 is formed at the interface close to the solder alloy, but planar Cu_5Zn_8 is located at the interface near to the Cu substrate. When heat-treated at 150°C for 200 h the IMCs morphology of the Sn-9Zn-1.5Ag/Cu is illustrated in Fig. 5(b), indicating that in addition to scallop-shaped Cu_6Sn_5 and planar Cu_5Zn_8 , planar Ag_3Sn is also formed at the interface close to the solder alloy.

Figure 5(c) demonstrates that the IMCs of the Sn-9Zn-1.5Ag-1Bi/Cu when dipped at 250°C for 60 s, are scallop-shaped Cu_6Sn_5 and planar Cu_5Zn_8 at the interface. Many reports have pointed out that Sn-Zn are not formed when a Cu substrate is dipped in a solder alloy.^{13,14,16)} Cu-Sn and Cu-Zn compounds are the best assembly in the Cu substrate and solder alloy system. The solubility of Bi in β -Sn is about 21 mass% at the eutectic temperature and about 2 mass% at room temperature, and has a solid solution strengthening effect.^{17,18)} Therefore, 1% Bi added to Sn-9Zn-1.5Ag solder

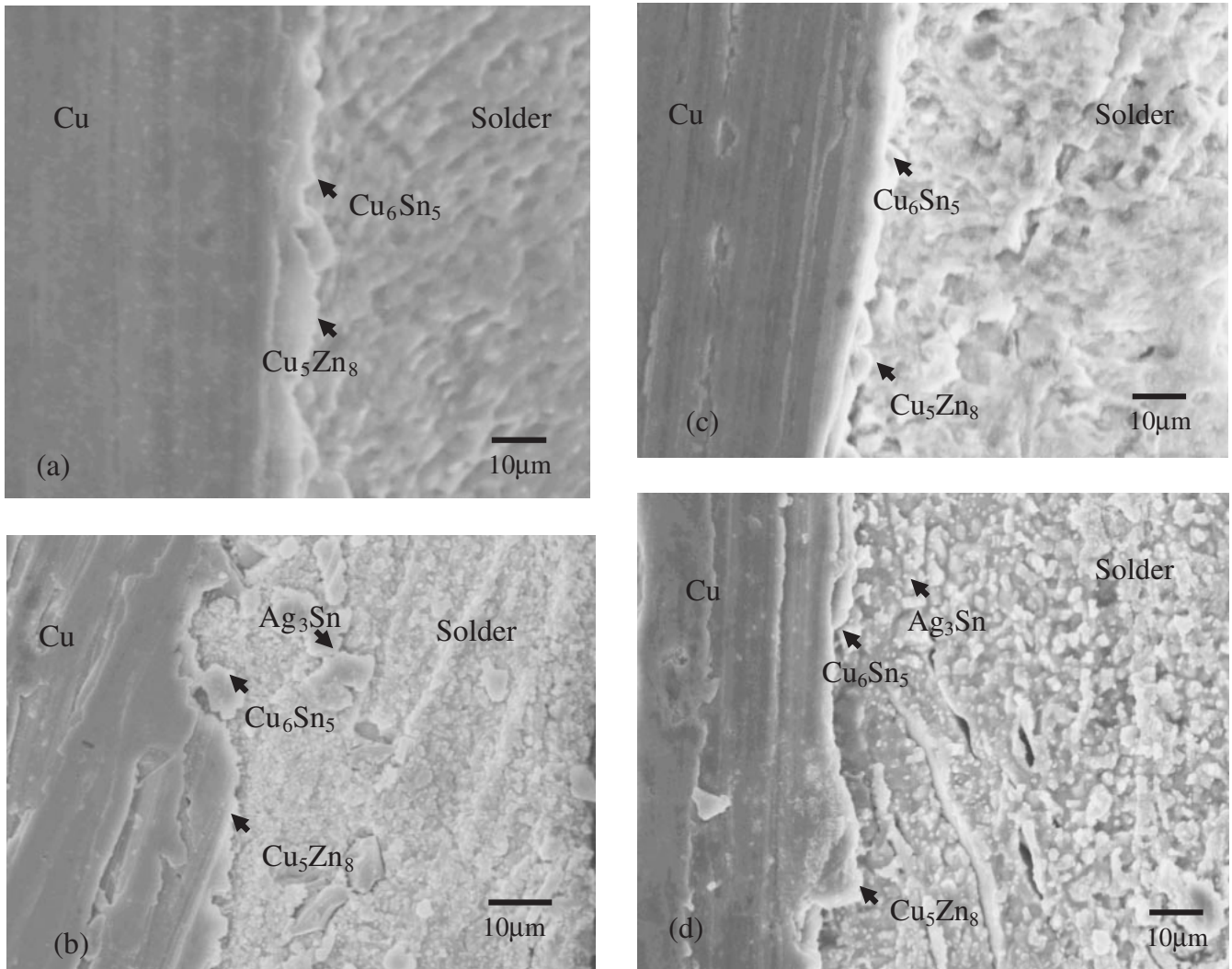


Fig. 5 SEM micrographs of Sn-9Zn-1.5Ag-xBi/Cu for (a) as-soldered Sn-9Zn-1.5Ag/Cu, (b) heat-treated at 150°C for 200 h of Sn-9Zn-1.5Ag/Cu, (c) as-soldered Sn-9Zn-1.5Ag-1Bi/Cu and (d) heat-treated at 150°C for 200 h of Sn-9Zn-1.5Ag-1Bi/Cu.

does not induce precipitation and remains in the solid solution. From Fig. 5(c), except for Cu_6Sn_5 and Cu_5Zn_8 , there is no Bi compound formed in the solder alloy.

The IMCs morphology of the Sn-9Zn-1.5Ag-1Bi/Cu when dipped at 250°C for 60 s and heat-treated at 150°C for 200 h is shown in Fig. 5(d). It indicates that in addition to Cu_6Sn_5 and Cu_5Zn_8 at the interface, the planar shape Ag_3Sn is also formed at the interface between the solder alloy and substrate. This is because the heat treatment provides energy and Ag is diffused to Sn to form Ag_3Sn . This result corresponds to the result of Fig. 3.

3.3 Effect of thermal treatment on the adhesion strength of the Sn-9Zn-1.5Ag-xBi ($x = 0$ and 1) lead-free solder alloys

The adhesion strength of the Sn-9Zn-1.5Ag/Cu and Sn-9Zn-1.5Ag-1Bi/Cu after being dipped at 250°C for 60 s and heat-treated at 150°C for various times is shown in Fig. 6. In the Sn-9Zn-1.5Ag/Cu, it is found that the maximum and minimum values of the adhesion strength are 8.17 ± 0.56 MPa and 5.12 ± 0.47 MPa for as-soldered and heat-treated at 150°C for 200 h, respectively. This result is caused by the

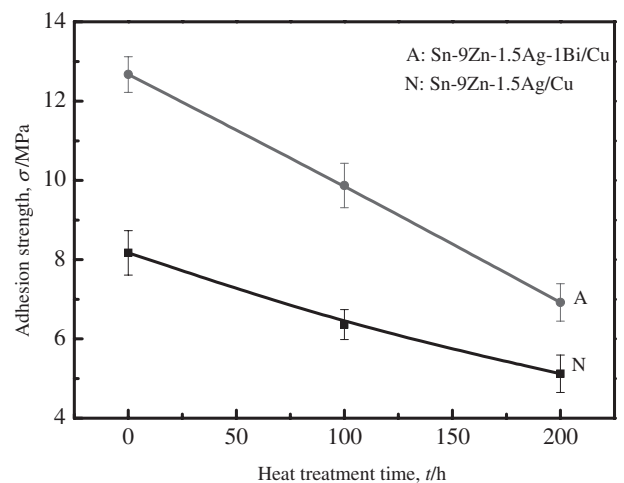


Fig. 6 Adhesion strength of Sn-9Zn-1.5Ag-xBi/Cu after dipped at 250°C for 60 s and heat-treated at 150°C for various times.

increase of the grain size with heat treatment time. Moreover, in the Sn-9Zn-1.5Ag-1Bi/Cu, Fig. 6 also illustrates the maximum and minimum adhesion strengths are $12.67 \pm$

0.45 MPa and 6.92 ± 0.38 MPa for as-soldered and heat-treatment at 150°C for 200 h, respectively. The decrease in adhesion strength after heat-treated is attributed to coarsening behavior and intermetallic growth response.¹⁹⁾

The adhesion strength of the Sn-9Zn-1.5Ag-1.5Bi solder alloy as-soldered, 12.67 ± 0.45 MPa, is larger than 8.17 ± 0.56 MPa of Sn-9Zn-1.5Ag/Cu. Furthermore, the adhesion strength, 6.92 ± 0.38 MPa, of the Sn-9Zn-1.5Ag-1Bi/Cu is larger than 5.12 ± 0.47 MPa of the Sn-9Zn-1.5Ag/Cu after heat-treatment at 150°C for 200 h. Therefore, the adhesion strength of the Sn-9Zn-1.5Ag-1Bi/Cu is larger than the Sn-9Zn-1.5Ag/Cu as-soldered and heat-treated at 150°C for 200 h. According to the results of Fig. 1(a) and (b), the wettability of the Sn-9Zn-1.5Ag-1Bi/Cu is better than Sn-9Zn-1.5Ag/Cu. Moreover, Suganamum *et al.*²⁰⁾ have also demonstrated the inferior wettability between Sn-9Zn solder alloy and Cu substrate. Bi addition to the Sn-9Zn-1.5Ag solder alloy has a better strength effect than the Sn-9Zn-1.5Ag solder alloy due to its solid solution strengthening effect.¹⁸⁾ Therefore, Sn-9Zn-1.5Ag-1Bi/Cu has better adhesion strength than Sn-9Zn-1.5Ag/Cu.

The fracture morphology of the Sn-9Zn-1.5Ag/Cu interface after being heat-treated at 150°C for 200 h is shown in Fig. 7(a). The fracture path is along the $\text{Cu}_6\text{Sn}_5/\text{Cu}_5\text{Zn}_8$ and Sn-9Zn-1.5Ag/ Ag_3Sn interface. It indicates that the bonding of the Sn-9Zn-1.5Ag/Cu interface is lower when heat-treated at 150°C for 200 h. According to Fig. 5(b), an incisive Cu_6Sn_5 layer is formed at the Sn-9Zn-1.5Ag/Cu interface and planar Ag_3Sn is formed near the Sn-9Zn-1.5Ag solder. Frear *et al.*²¹⁾ have pointed out that failure located close to the interface may result from the stress concentration at or adjacent to the interface of the solder alloy/IMCs interface, which is caused by the plastic inhomogeneity between the substrate and solder alloy. Two possible reasons are (i) stress concentration and (ii) Sn-depletion zone formation during soldering and heat-treatment. Moreover, Yu *et al.*²²⁾ have also reported that the decrease of adhesion strength of the Sn-Zn-Al/Cu substrate is due to the different coefficients of thermal expansion, causing thermal stress at the interface between the Al, Zn-rich and Sn-rich phases.

Figure 7(b) shows the fracture morphology of the Sn-9Zn-1.5Ag-1Bi/Cu interface when dipped at 250°C for 60 s and heat-treated at 150°C for 200 h, which indicates that the fracture occurs at the Sn-9Zn-1.5Ag-1Bi/ Cu_5Zn_8 and $\text{Cu}_6\text{Sn}_5/\text{Sn-9Zn-1.5Ag-1Bi}$ interfaces. However, Cu_5Zn_8 offers a better bonding strength than Cu_6Sn_5 , thus, for the Sn-9Zn-1.5Ag-1Bi/Cu interface, fracture occurring at the $\text{Cu}_6\text{Sn}_5/\text{Sn-9Zn-1.5Ag-1Bi}$ interface is a dominant factor.

On the other hand, the adhesion strength of the Sn-9Zn-1.5Ag/Cu interface decreases from 8.17 ± 0.56 to 5.12 ± 0.47 MPa when heat-treatment time increases from 0 to 200 h. Microvoids do not form at the $\text{Cu}_6\text{Sn}_5/\text{Cu}_5\text{Zn}_8$ interface after heat-treatment. Chang *et al.*¹²⁾ have pointed out that Kirkendall voids are not found at the Sn-9Zn-xAg/Cu interface when aged at 150°C for 750 h, and the adhesion strength decrease after heat-treatment is due to the grain growth. Figure 4 also shows that the Sn-9Zn-1.5Ag-xBi/Cu has the largest grain size after being heat-treated at 150°C for 200 h.

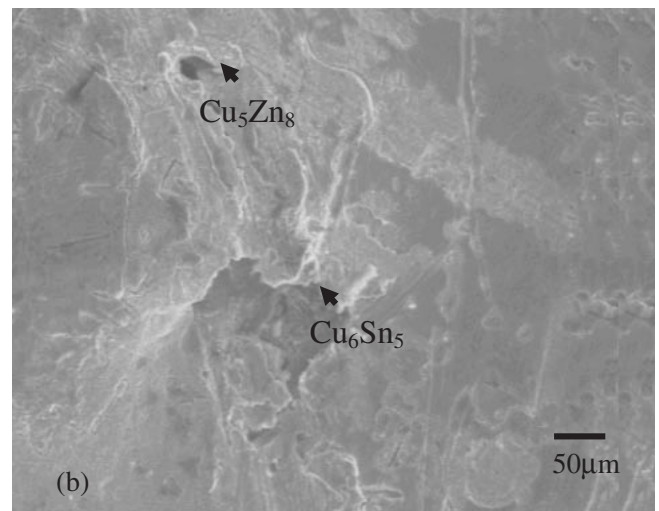
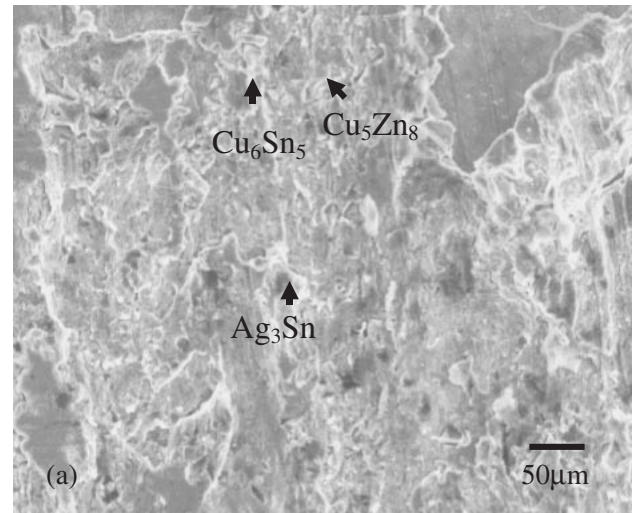


Fig. 7 Fractographs of Sn-9Zn-1.5Ag-xBi/Cu heat-treated at 150°C for 200 h: (a) Sn-9Zn-1.5Ag/Cu and (b) Sn-9Zn-1.5Ag-1Bi/Cu interface.

4. Conclusions

The effects of the thermal treatment on the IMCs formed at the interface between the Sn-9Zn-1.5Ag-xBi lead-free solder and Cu substrate have been investigated by OM, XRD, SEM and EDS. Sn-9Zn-1.5Ag-1Bi lead-free solder alloy has better wettability than Sn-9Zn-1.5Ag due to Bi addition, which increases the mobility of the solder alloy on the Cu substrate. Cu_6Sn_5 and Cu_5Zn_8 are the IMCs phases formed between the solder alloy and Cu substrate after dipping. After thermal treatment at 150°C for 200 h, Ag_3Sn is also formed at the interface between solder alloy and Cu substrate. The morphology of Cu_6Sn_5 IMCs is scallop-shaped at the interface near the Cu substrate. Adhesion strength decreases from 12.67 ± 0.45 to 6.92 ± 0.38 MPa for Sn-9Zn-1.5Ag-1Bi/Cu, and 8.17 ± 0.56 to 5.12 ± 0.47 MPa for Sn-9Zn-1.5Ag/Cu heat-treated at 150°C for 0~200 h, respectively.

Acknowledgements

This work was supported by the National Science Council of Taiwan under Contract No. NSC89-2216-E-151-011 and

NSC95-2221-E-151-007, which is gratefully acknowledged. Experimental assistance and suggestions from Mr. H. Y. Hwang and Prof. M. P. Hung are sincerely appreciated.

REFERENCES

- 1) M. L. Huang, T. Loehner, A. Ostmann and H. Reichl: *Appl. Phys. Lett.* **86** (2005) 181908–181910.
- 2) H. K. Kim and K. N. Tu: *Phys. Rev.* **B53** (1996) 16027–16034.
- 3) G. Ghosh: *Metall. Mater. Trans.* **A30** (1999) 1481–1494.
- 4) X. J. Liu, M. Kinaka, Y. Takaku, I. Ohnuma, R. Kainuma and K. Ishida: *J. Electron. Mater.* **34** (2005) 670–679.
- 5) I. Shohji, T. Yoshida, T. Takahashi and S. Hioki: *Mater. Trans.* **43** (2002) 1854–1857.
- 6) C. B. Lee, S. B. Jung, Y. E. Shin and C. C. Shur: *Mater. Trans.* **42** (2001) 751–755.
- 7) S. Chada, W. Laub, R. A. Fourelle and D. Shangguan: *J. Electron. Mater.* **28** (1999) 1194–1202.
- 8) J. Sigelko, S. Choi, K. N. Subramanian, J. P. Lucas and T. R. Bieler: *J. Electron. Mater.* **28** (1999) 1184–1188.
- 9) T. Takemoto and T. Funaki: *Mater. Trans.* **43** (2002) 1784–1790.
- 10) T. C. Chang, M. C. Wang and M. H. Hon: *J. Crystal Growth* **252** (2003) 391–400.
- 11) M. O. Alam, Y. C. Chan and K. N. Tu: *J. Appl. Phys.* **94** (2003) 7904–7909.
- 12) T. C. Chang, M. C. Wang and M. H. Hon: *J. Crystal Growth* **250** (2003) 236–243.
- 13) C. Y. Liu, M. C. Wang and M. H. Hon: *J. Electron. Mater.* **33** (2004) 1557–1560.
- 14) J. Glazer: *Int. Mater. Rev.* **40** (1995) 65–96.
- 15) B. D. Cullity: *Elements of X-ray Diffraction*, 2nd Edition, Addison-Wesley Publishing Company (1978) pp. 248.
- 16) T. C. Chang, M. H. Hon, M. C. Wang and D. Y. Lin: *J. Electrochem. Soc.* **151** (2004) C484–C491.
- 17) G. Ghosh: *J. Electron. Mater.* **28** (1999) 1238–1250.
- 18) B. Y. Wu, Y. C. Chan, M. O. Alam and W. Jillek: *J. Mater. Res.* **21** (2006) 62–70.
- 19) S. S. A. E. Rehim, H. H. Hassan and N. F. Mohamed: *Corr. Sci.* **46** (2004) 1071–1082.
- 20) K. Suganuma, K. Niihara, T. Shoutoku and Y. Nakamura: *J. Mater. Res.* **13** (1998) 2859–2865.
- 21) D. R. Frear, S. N. Burchett, H. S. Morgan and J. H. Lau: *The Mechanics of Solder Alloy Interconnects* (New York: Van Nostrand Reinhold, 1994) pp. 62.
- 22) S. P. Yu, M. C. Wang and M. H. Hon: *J. Mater. Res.* **16** (2001) 76–82.